PROCEEDINGS OF SCIENCE

Latest results from the searches for ultra-high-energy photons at the Pierre Auger Observatory

Pierpaolo Savina[ab,*] **for the Pierre Auger Collaboration**[c]

[a] *Gran Sasso Science Institute (GSSI), Via Iacobucci 2, I-67100 L'Aquila, Italy*

[b] *Istituto Nazionale di Fisica Nucleare (INFN) - Laboratori Nazionali del Gran Sasso, Via G. Acitelli 22, I-67100 Assergi, L'Aquila, Italy*

[c] *Observatorio Pierre Auger, Av. San Martín Norte 304, 5613 Malargüe, Argentina*

Full author list: https://www.auger.org/archive/authors_icrc_2025.html

E-mail: spokespersons@auger.org

The Pierre Auger Observatory is the largest air-shower detector in the world, offering unparalleled exposure to photons with energies above 5×10^{16} eV. Since the start of data collection almost two decades ago, numerous searches for photons have been conducted using the detection systems of the Observatory. These searches have led to the most stringent upper limits on the diffuse photon flux. These limits place severe constraints on current models regarding the origin of ultra-high-energy cosmic rays and emphasize the significant capabilities of the Pierre Auger Observatory in the context of multimessenger astronomy at the highest energies. This contribution provides an overview of the ongoing efforts to search for high-energy photons in the data from the Pierre Auger Observatory. The latest results from searches for the diffuse photon flux will be presented, along with follow-up investigations for photons associated with transient events, such as gravitational wave detections. Furthermore, future prospects will be discussed in light of the ongoing AugerPrime detector upgrade, which will enhance the sensitivity of the Observatory to photons up to the highest energies.

39th International Cosmic Ray Conference (ICRC2025)
15 – 24 July, 2025
Geneva, Switzerland

ICRC 2025
The Astroparticle Physics Conference
Geneva July 15-24, 2025

*Speaker

PoS(ICRC2025)965

1. Introduction

The search for ultra-high-energy (UHE) photons of cosmic origin is one of the primary scientific goals of the Pierre Auger Observatory. While no UHE photons have been unambiguously identified to date, the upper limits on their flux have already placed strong constraints. The detection of UHE photons would be of fundamental importance for advancing the multimessenger approach to understanding the most extreme astrophysical phenomena. Unlike charged particles, neutral messengers such as photons point back directly to their sources, offering valuable directional information. However, unlike neutrinos, UHE photons interact with the background photon fields that permeate the Universe. These interactions significantly reduce their attenuation length to about 30 kpc at 10^{15} eV amd approximately 10 Mpc at 10^{19} eV.

In this contribution, we review the current status of UHE photon searches at the Pierre Auger Observatory. After a brief overview of the characteristics of photon-induced air showers (Sec. 2), we describe the Pierre Auger Observatory and its detection capabilities (Sec. 3). We then focus on the search for a diffuse flux of UHE photons using the Observatory's various detector systems (Sec. 4), followed by searches for UHE photons originating from transient events (Sec. 5).

2. Photon-induced air Showers

There are two principal physical differences between air showers initiated by photons and those initiated by hadrons [1]: first, the longitudinal development of a photon-induced air shower is delayed compared to that of hadron-induced showers. This delay arises from the lower multiplicity of electromagnetic interactions—which dominate in photon showers—relative to hadronic interactions. As a result, the atmospheric depth at which the number of shower particles reaches its maximum, $X_{\max}$, is typically greater for photon-induced showers. Moreover, due to the much larger mean free path for photo-nuclear interactions compared to the radiation length, only a small fraction of the electromagnetic component in a photon-induced shower is converted into the hadronic component, and subsequently into muons. As a result, these showers contain significantly fewer muons than hadron-induced showers of the same primary energy. All searches for UHE photons using air-shower data are based on these two distinguishing features. $X_{\max}$ can be measured directly via the air-fluorescence technique. Although the water Cherenkov detectors of the Pierre Auger Observatory cannot yet directly measure the number of muons, it is possible to infer information about the muonic content by studying the lateral distribution of secondary particles at ground level. The steepness of this lateral distribution depends on both the muon number and the shower development profile, and is sensitive to the type of primary particle.

3. The Pierre Auger Observatory

The Pierre Auger Observatory [2] is the largest cosmic-ray observatory currently in operation, offering unprecedented exposure to UHE photons. A defining feature of the Observatory is its hybrid detection strategy, which combines a Surface Detector array (SD) with a Fluorescence Detector (FD). The SD consists of 1600 water-Cherenkov detectors arranged on a triangular grid with 1500 m spacing (referred to as SD-1500), covering an area of approximately 3000 km^2.

Surrounding the array at four peripheral sites are 24 fluorescence telescopes that constitute the FD. While the SD continuously samples the lateral distribution of shower particles at ground level with an almost 100% duty cycle, the FD records the longitudinal development of extensive air showers in the atmosphere. However, the FD operates only during clear, moonless nights, limiting its duty cycle to about 15%. By combining data from both systems in so-called hybrid events, the Pierre Auger Observatory achieves superior accuracy in reconstructing air-shower parameters compared to using either system alone. To extend the sensitivity of the Observatory to lower energies (below 10^{18} eV), two denser infill sub-arrays have been deployed in the western section of the SD: **SD-750**, composed of 50 additional detectors placed between the standard SD-1500 stations with 750 m spacing, covering an area of approximately 27.5 km^2, and **SD-433**, a smaller sub-array consisting of 10 detectors with 433 m spacing, primarily used for calibration and dedicated low-energy studies. To enable hybrid measurements in this lower-energy regime, where air showers typically develop higher in the atmosphere beyond the field of view of the standard FD telescopes, the SD-750 sub-array is operated in conjunction with the High-Elevation Auger Telescopes (HEAT) installed at the Coihueco FD site. The HEAT telescopes observe the atmosphere at elevation angles from 30° to 60°, complementing the original Coihueco telescopes, which cover the range from 0° to 30°.

4. Searches for a diffuse flux of photons

In this section, we summarize the four most recent diffuse, i.e. direction-independent, unresolved, photon searches conducted at the Pierre Auger Observatory, ordered by increasing energy range. At $E > 5 \times 10^{16}$ eV, a dedicated analysis using underground muon detectors (UMD) and the SD-433 has been performed [5]. In the range 2×10^{17} eV $< E < 10^{18}$ eV, a low-energy hybrid analysis combining $X_{\rm max}$ and SD observables was carried out [6]. At $E > 10^{18}$ eV, an updated hybrid analysis was used [7], while for $E > 10^{19}$ eV, photon-induced air showers were searched for using SD data only [3].

4.1 Energy range $E > 5 \times 10^{16}$ eV

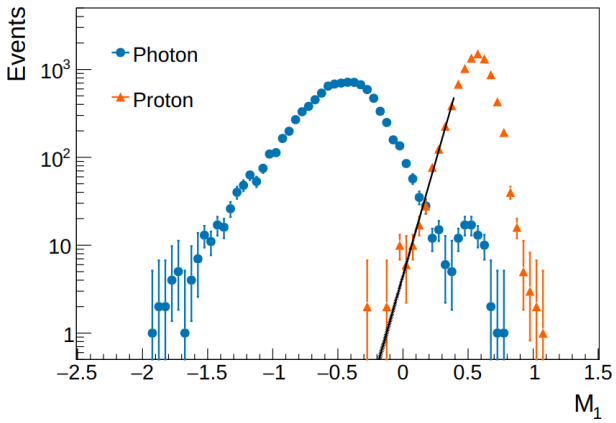

Figure 1: Distributions of M_1 for simulated photon- and proton-induced events in the energy range $\log_{10}(E_{\gamma,\rm eq}/\rm eV) \in (16.7, 16.9)$. Uncertainties in bins with fewer than ten entries correspond to 95% confidence intervals using the Feldman–Cousins method. The black band shows the fit to the proton tail used to estimate background contamination. See details in [5].

The photon search above 5×10^{16} eV exploits the low muon content of electromagnetic air showers, using signals from the UMD. A muon-based observable, $M_b = \log_{10}\left(\sum_i \frac{\rho_i}{\rho_{\rm pr}} \left(\frac{r_i}{r_{\rm pr}}\right)^b\right)$, is

constructed from the muon densities ρ_i at stations i, normalized to the average proton-induced muon density $\rho_{\rm pr}$ at a reference distance $r_{\rm pr} = 200$ m. This normalization absorbs energy and zenith-angle dependencies, where $\rho_{\rm pr}$ is obtained from simulations. To suppress fluctuations from peripheral stations, M_b is computed using only the six detectors around the station with the highest signal. The parameter b is optimized for photon-hadron separation, yielding $b = 1$ and defining the final observable M_1. Photon-induced showers typically yield lower M_1 values, while muon-rich proton showers dominate the background.

As shown in Fig. 1, the M_1 distributions show a clear but non-perfect separation: rare muon-poor proton events and photonuclear interactions may cause overlap. A conservative estimate of background contamination is derived by fitting the lower tail of the proton M_1 distribution, while signal efficiency is defined relative to photon simulations. This approach enables a tunable trade-off between efficiency and contamination, crucial for rare photon searches. Upper limits on the integral photon flux $\Phi_\gamma^{\rm UL}(E_\gamma > E_0)$ at 95% confidence level are derived for threshold energies of 50, 80, 120, and 200 PeV. The resulting upper limits on the integral flux are 12.3, 11.7, 11.3, and 11.3 $\rm km^{-2}\,sr^{-1}\,yr^{-1}$, respectively [5].

4.2 Energy range 2×10^{17} eV < E < 10^{18} eV

The photon search in the energy range, starting at 2×10^{17} eV [6], uses data from the SD-750 array combined with HEAT and Coihueco telescopes (HeCo). Three observables are used in a multivariate analysis based on Boosted Decision Trees (BDT): $X_{\rm max}$ (from FD), the signal-based parameter $S_b = \sum_i S_i (r_i/1000\ {\rm m})^b$ with $b = 4$ (sensitive to shower development and muon content), and $N_{\rm stations}$, the number of triggered SD detectors. Simulated samples of primary photons (signal) and protons (background) are used for training and performance evaluation. The BDT includes also E_γ (calorimetric energy with 1% correction for missing energy) and the reconstructed zenith angle θ.

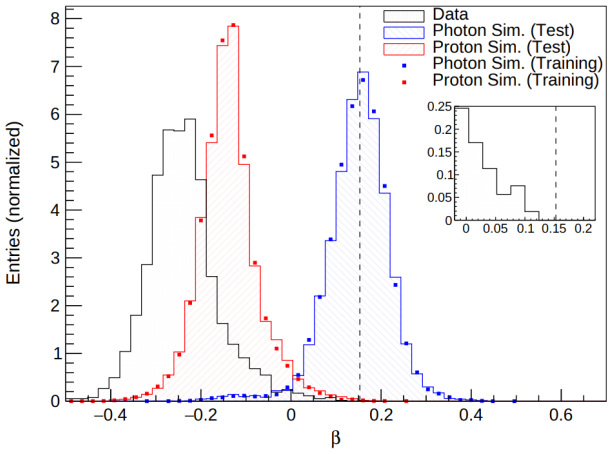

Figure 2: Distribution of simulated photons (blue), simulated protons (red), and data (black) of the BDT discriminator, β, combining $X_{\rm max}$, S_b, number of stations, photon energy, and zenith. The selection threshold for photon candidates is shown by the dashed line.

The analysis was applied to hybrid HeCo+SD-750 data collected from June 2010 to December 2015, yielding 2204 selected events above 2×10^{17} eV. No photon candidates are found above the BDT cut (50% signal efficiency), with a background rejection of (99.91 ± 0.03)%. Upper limits on the integral photon flux at 95% CL are derived assuming a E^{-2} spectrum and an efficiency-weighted exposure of 2.4–2.7 $\rm km^2\,sr\,yr$. The limits are 2.72, 2.50, 2.74, and 3.55 $\rm km^{-2}\,sr^{-1}\,yr^{-1}$ for threshold energies of 2, 3, 5×10^{17} eV, and 10^{18} eV, respectively. These translate to upper limits on the photon fraction of 0.28%, 0.63%, 2.20%, and 13.8% [6].

4.3 Energy range E > 10^{18} eV

The photon search at energies above 10^{18} eV [7] is performed using hybrid events. As in the lower-energy analysis, $X_{\max}$ is obtained from FD measurements, while the muon content of air showers is quantified by the parameter F_μ, derived from SD signals using air-shower universality [7].

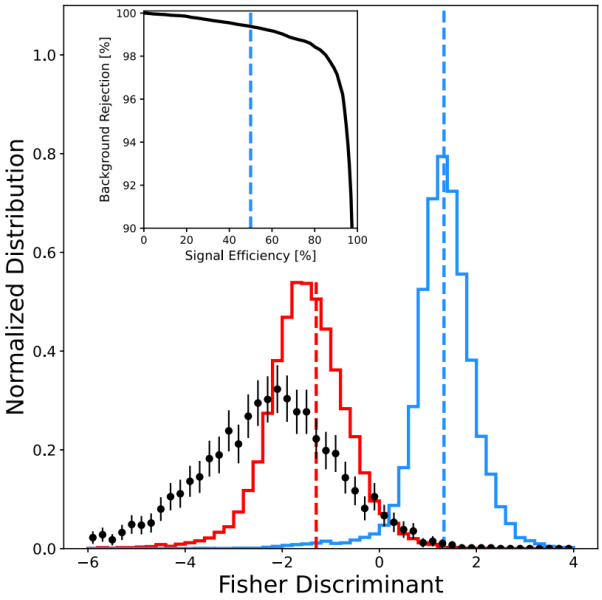

Figure 3: Distribution of the Fisher discriminant for simulated photons (signal, blue), protons (background, red), and for the burnt sample (black). The vertical red line marks the threshold $f = -1.3$, above which the background decreases nearly exponentially while the photon selection efficiency remains close to 100%. The blue line indicates the median of the photon distribution. Inset: background rejection as a function of signal efficiency from the Fisher discriminant analysis.

F_μ is a proxy of the muon content of the shower. it is derived for each hybrid event by matching the observed SD signals to the signal predicted by the universality model. Combined with $X_{\max}$ and the photon-estimated energy E_γ, F_μ is used in a linear Fisher discriminant analysis to separate photons from hadrons (Fig. 3). The Fisher discriminant f shows strong separation between simulated photon and proton events. A 5% burnt sample of data is used to estimate the background. Due to limited statistics, only events with $f > -1.3$ are used to model the tail of the background, which is then fitted and scaled to the full data set (2005–2017, ~32,000 hybrid events above 10^{18} eV). After applying the photon selection cut (at the median of the photon f distribution), 22 photon candidates are identified, consistent with the background expectation of 30 ± 15 events. Upper limits on the integral photon flux $\Phi_\gamma^{\rm UL}(E_\gamma > E_0)$ at 95% CL are set for thresholds of 1, 2, 3, 5×10^{18} eV, and 10^{19} eV. The number of photon candidates observed for each threshold is 22, 2, 0, 0, and 0, respectively. These are compatible with the background expectations 30 ± 15, 6 ± 6, 0.7 ± 1.9, 0.06 ± 0.25, and 0.02 ± 0.06. The efficiency-weighted exposure, derived from simulations assuming a E^{-2} spectrum, ranges from 420.7 to 1245.9 km^2 sr yr. The resulting upper limits on the integral photon flux are: 4.0, 1.1, 0.35, 0.23, and 0.0021 km^{-2} sr^{-1} yr^{-1} [7].

4.4 Energy range E > 10^{19} eV

At energies above 10^{19} eV, the data collected by the SD-1500 are considered. While the high duty cycle of the SD provides a large exposure, the absence of FD measurements poses challenges, particularly for the determination of $X_{\max}$. Two observables are employed for photon-hadron discrimination: one related to the thickness of the shower front, and one based on the steepness of the lateral distribution. The first observable, Δ, is derived from the risetime $t_{1/2}$ in individual SD stations—the time interval in which the integrated signal rises from 10% to 50%

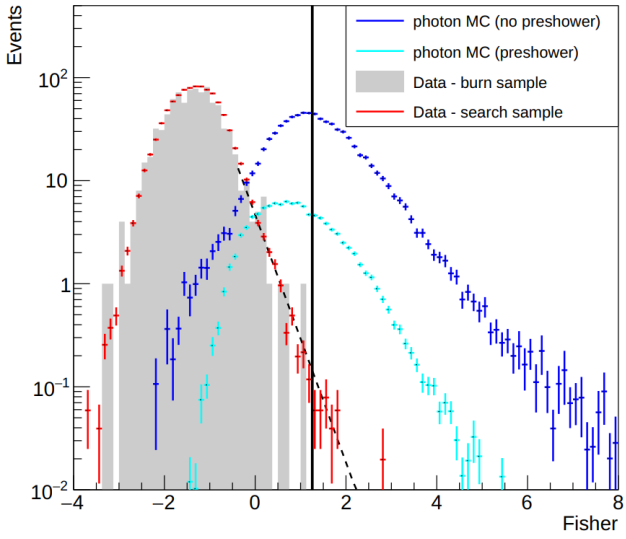

Figure 4: Distributions of the Fisher discriminant for the burnt sample (grey), the search sample (red), and simulated primary photons—non-preshowering (blue) and preshowering (light blue)—weighted with an E^{-2} spectrum. The search and photon distributions are rescaled to match the integral of the burnt sample. The vertical line indicates the photon-candidate cut. The dashed line represents an exponential fit to the top 5% of events in the burnt sample with the highest Fisher discriminant values. See details in [3].

of its total value. Photon-induced showers typically exhibit longer risetimes due to their lower muon content and deeper development in the atmosphere. The second observable, L_{LDF}, quantifies the steepness of the lateral distribution function (LDF) of the signal. The two observables are combined into a Fisher discriminant. The analysis is applied to SD data collected between 1 January 2004 and 30 June 2020, including only events with zenith angles between 30° and 60° to ensure full shower development before ground. After applying quality cuts [3], the search sample includes 48,061 events with $E_\gamma \geq 10^{19}$ eV; a burnt sample of 886 events (1.8%) is used to estimate the background. Applying the photon-candidate cut (defined as the median of the Fisher distribution for simulated non-preshowering photons), 16, 2, and 0 events are observed above 1, 2, and 4×10^{19} eV, respectively. These results are consistent with expectations from an exponential fit to the tail of the burn-sample Fisher distribution. No excess or peak-like feature indicative of a photon signal is observed. Upper limits on the integral photon flux are derived at 95% CL, using simulation-based signal efficiencies that increase from 0.26 to 0.39 for thresholds between 10^{19} eV and 4×10^{19} eV. The resulting upper limits on the photon flux are: $2.11 \times 10^{-3}\,\mathrm{km^{-2}\,sr^{-1}\,yr^{-1}}$ for $E_\gamma > 10^{19}$ eV, $0.312 \times 10^{-3}\,\mathrm{km^{-2}\,sr^{-1}\,yr^{-1}}$ for $E_\gamma > 2 \times 10^{19}$ eV, and $0.172 \times 10^{-3}\,\mathrm{km^{-2}\,sr^{-1}\,yr^{-1}}$ for $E_\gamma > 4 \times 10^{19}$ eV.

4.5 Results from the diffuse analyses

The upper limits on the integral photon flux obtained from the four analyses (see Fig. 5) represent the most stringent constraints to date across 2×10^{16} eV to the highest energies. The results are robust against systematic uncertainties. Fig. 5 also compares expectations from cosmogenic photons (proton and mixed-composition models), Galactic interactions, and super-heavy dark matter (SHDM) decay. Current limits start to constrain optimistic proton scenarios, while SHDM models remain viable only within specific mass–lifetime combinations.

5. Follow-up studies to transient events

Detecting UHE photons from distant sources poses considerable challenges. The flux is expected to be strongly attenuated through interactions with cosmic background radiation fields,

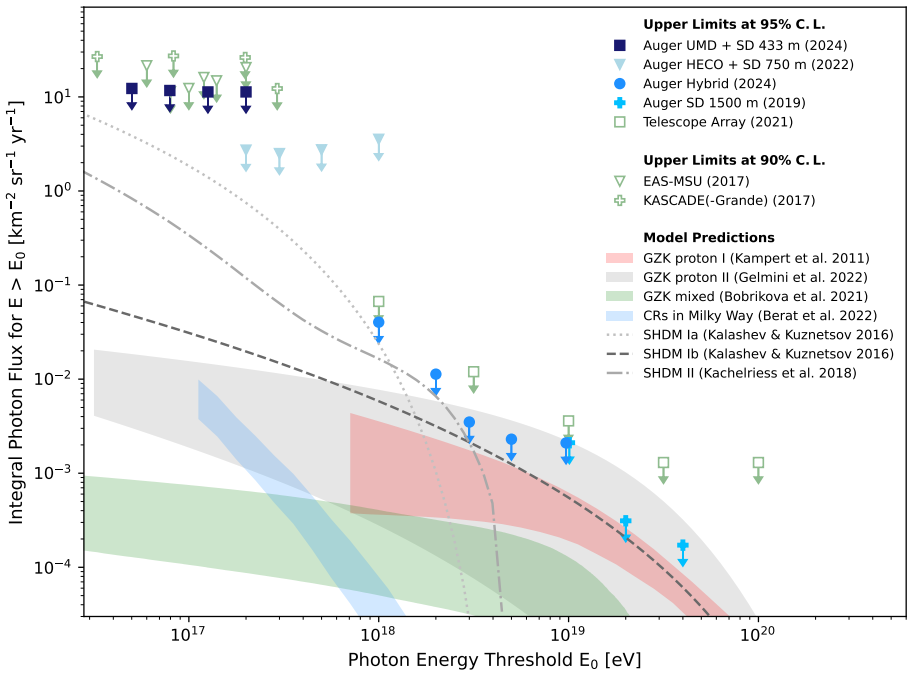

Figure 5: Upper limits on the integral photon flux above threshold energy $E_\gamma^{\rm th}$ from this work (red markers, 95% CL) and previous Pierre Auger results at higher energies (blue and black markers, 95% CL), alongside limits from other experiments (90% CL, except Telescope Array at 95%). Shaded bands show cosmogenic flux predictions from UHECR interactions with galactic matter (gray), background radiation fields (violet, green, orange), and hot gas in the galactic halo (blue). Dashed lines denote super-heavy dark matter predictions (more details in [5]).

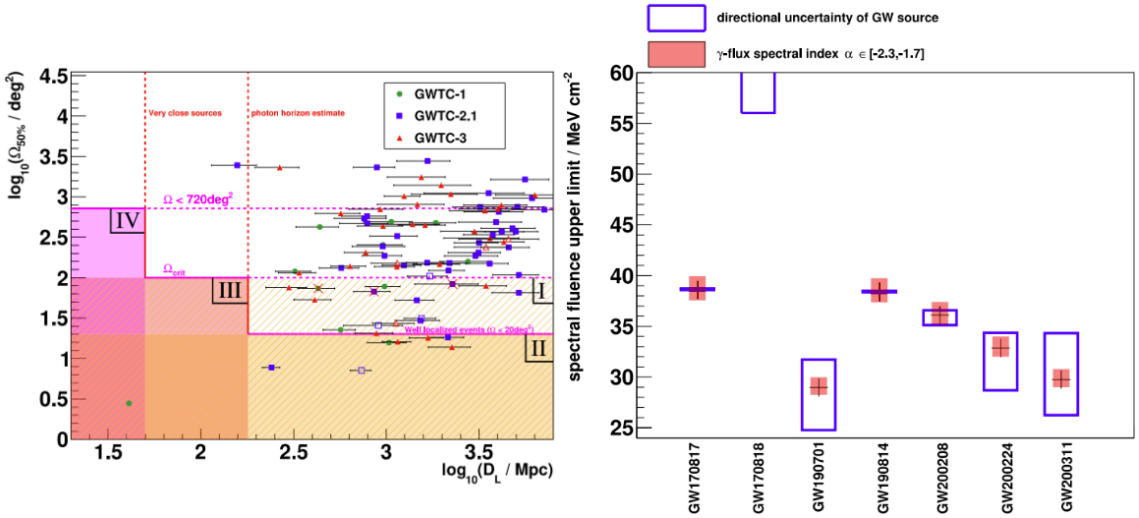

Figure 6: Left: Three classes of gravitational wave sources in the photon follow-up search, defined by their 50% localization region ($\Omega_{50\%}$) and luminosity distance (D_L). Circled markers indicate events overlapping with the SD field of view. Right: Upper limits on the spectral fluence of UHE photons at Earth for each source; error bars include directional uncertainty (blue) and spectral index uncertainty (red). For the second event, error bars exceed the plot range due to its position near the SD field of view edge [8].

and air showers initiated by hadronic cosmic rays create a substantial background that complicates unambiguous photon identification. Photon candidate events are selected using standard criteria [3] applied to SD-1500 data. To maximize sensitivity to transient photon sources while suppressing background, a dedicated selection strategy has been developed for gravitational wave follow-up. This strategy accepts only GW events that are either nearby or well-localized on the sky. Three classes of acceptable GW events are defined in the plane of 50% sky localization region versus luminosity distance. Nearby sources are most likely to produce detectable UHE photons, but the detection of photons from distant, well-localized events could indicate physics beyond the Standard Model. From the GWTC-1 and GWTC-2 catalogs, 10 gravitational wave events—including GW170817, associated with a neutron star merger and a coincident short gamma-ray burst were selected for targeted photon searches. The analysis covered a time window of one sidereal day following each GW event. No photon candidate events were detected. A similar search strategy was applied to investigate potential UHE photon emission associated with other transient sources, such as the blazar TXS 0506+056. No photon candidates were observed during either of the two periods of enhanced neutrino activity reported by IceCube: October 2014–February 2015 and March–September 2017. At gigaparsec distances, the non-detection of UHE photons is consistent with expectations based on standard photon propagation models. The observation of such photons would likely require new physics, such as reduced photon attenuation in the extragalactic medium.

6. Conclusions

The Pierre Auger Observatory provides unmatched exposure to ultra-high energy (UHE) cosmic rays, photons. It has set the most stringent upper limits on diffuse UHE photon fluxes and performed targeted searches in coincidence with gravitational waves and other transients, reinforcing its role in multimessenger astronomy at the highest energies. The ongoing upgrade, *AugerPrime*, will enhance these capabilities. Scintillator detectors are being added to each surface station to improve shower component separation and composition sensitivity. The stations are also being equipped with radio antennas, and upgraded electronics allow for improved timing and dynamic range. These developments will strengthen the Observatory's ability to detect or further constrain UHE photons.

References

[1] M. Risse and P. Homola, Mod. Phys. Lett. A 22 (2007) 749

[2] A. Aab et al. [Pierre Auger Coll.], Nucl. Instrum. Meth. A 798 (2015) 172.

[3] P. Abreu et al. [Pierre Auger Coll.], JCAP 05 (2023) 021.

[4] P. Abreu et al. [Pierre Auger Coll.], Universe 8 (2022) 579.

[5] A. Abdul Halim et al. [Pierre Auger Coll.], JCAP 05 (2025) 061.

[6] P. Abreu et al. [Pierre Auger Coll.] Astrophys. J. 933 (2022) 125.

[7] A. Abdul Halim et al. [Pierre Auger Coll.], Phys. Rev. D 110, 062005

[8] A. Abdul Halim et al. [Pierre Auger Coll.] Astrophys. J. 952 (2023) 91

The Pierre Auger Collaboration

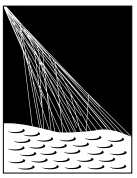

A. Abdul Halim[13], P. Abreu[70], M. Aglietta[53,51], I. Allekotte[1], K. Almeida Cheminant[78,77], A. Almela[7,12], R. Aloisio[44,45], J. Alvarez-Muñiz[76], A. Ambrosone[44], J. Ammerman Yebra[76], G.A. Anastasi[57,46], L. Anchordoqui[83], B. Andrada[7], L. Andrade Dourado[44,45], S. Andringa[70], L. Apollonio[58,48], C. Aramo[49], E. Arnone[62,51], J.C. Arteaga Velázquez[66], P. Assis[70], G. Avila[11], E. Avocone[56,45], A. Bakalova[31], F. Barbato[44,45], A. Bartz Mocellin[82], J.A. Bellido[13], C. Berat[35], M.E. Bertaina[62,51], M. Bianciotto[62,51], P.L. Biermann[a], V. Binet[5], K. Bismark[38,7], T. Bister[77,78], J. Biteau[36,i], J. Blazek[31], J. Blümer[40], M. Boháčová[31], D. Boncioli[56,45], C. Bonifazi[8], L. Bonneau Arbeletche[22], N. Borodai[68], J. Brack[f], P.G. Brichetto Orchera[7,40], F.L. Briechle[41], A. Bueno[75], S. Buitink[15], M. Buscemi[46,57], M. Büsken[38,7], A. Bwembya[77,78], K.S. Caballero-Mora[65], S. Cabana-Freire[76], L. Caccianiga[58,48], F. Campuzano[6], J. Caraça-Valente[82], R. Caruso[57,46], A. Castellina[53,51], F. Catalani[19], G. Cataldi[47], L. Cazon[76], M. Cerda[10], B. Čermáková[40], A. Cermenati[44,45], J.A. Chinellato[22], J. Chudoba[31], L. Chytka[32], R.W. Clay[13], A.C. Cobos Cerutti[6], R. Colalillo[59,49], R. Conceição[70], G. Consolati[48,54], M. Conte[55,47], F. Convenga[44,45], D. Correia dos Santos[27], P.J. Costa[70], C.E. Covault[81], M. Cristinziani[43], C.S. Cruz Sanchez[3], S. Dasso[4,2], K. Daumiller[40], B.R. Dawson[13], R.M. de Almeida[27], E.-T. de Boone[43], B. de Errico[27], J. de Jesús[7], S.J. de Jong[77,78], J.R.T. de Mello Neto[27], I. De Mitri[44,45], J. de Oliveira[18], D. de Oliveira Franco[42], F. de Palma[55,47], V. de Souza[20], E. De Vito[55,47], A. Del Popolo[57,46], O. Deligny[33], N. Denner[31], L. Deval[53,51], A. di Matteo[51], C. Dobrigkeit[22], J.C. D'Olivo[67], L.M. Domingues Mendes[16,70], Q. Dorosti[43], J.C. dos Anjos[16], R.C. dos Anjos[26], J. Ebr[31], F. Ellwanger[40], R. Engel[38,40], I. Epicoco[55,47], M. Erdmann[41], A. Etchegoyen[7,12], C. Evoli[44,45], H. Falcke[77,79,78], G. Farrar[85], A.C. Fauth[22], T. Fehler[43], F. Feldbusch[39], A. Fernandes[70], M. Fernandez[14], B. Fick[84], J.M. Figueira[7], P. Filip[38,7], A. Filipčič[74,73], T. Fitoussi[40], B. Flaggs[87], T. Fodran[77], A. Franco[47], M. Freitas[70], T. Fujii[86,h], A. Fuster[7,12], C. Galea[77], B. García[6], C. Gaudu[37], P.L. Ghia[33], U. Giaccari[47], F. Gobbi[10], F. Gollan[7], G. Golup[1], M. Gómez Berisso[1], P.F. Gómez Vitale[11], J.P. Gongora[11], J.M. González[1], N. González[7], D. Góra[68], A. Gorgi[53,51], M. Gottowik[40], F. Guarino[59,49], G.P. Guedes[23], L. Gülzow[40], S. Hahn[38], P. Hamal[31], M.R. Hampel[7], P. Hansen[3], V.M. Harvey[13], A. Haungs[40], T. Hebbeker[41], C. Hojvat[d], J.R. Hörandel[77,78], P. Horvath[32], M. Hrabovský[32], T. Huege[40,15], A. Insolia[57,46], P.G. Isar[72], M. Ismaiel[77,78], P. Janecek[31], V. Jilek[31], K.-H. Kampert[37], B. Keilhauer[40], A. Khakurdikar[77], V.V. Kizakke Covilakam[7,40], H.O. Klages[40], M. Kleifges[39], J. Köhler[40], F. Krieger[41], M. Kubatova[31], N. Kunka[39], B.L. Lago[17], N. Langner[41], N. Leal[7], M.A. Leigui de Oliveira[25], Y. Lema-Capeans[76], A. Letessier-Selvon[34], I. Lhenry-Yvon[33], L. Lopes[70], J.P. Lundquist[73], M. Mallamaci[60,46], D. Mandat[31], P. Mantsch[d], F.M. Mariani[58,48], A.G. Mariazzi[3], I.C. Mariş[14], G. Marsella[60,46], D. Martello[55,47], S. Martinelli[40,7], M.A. Martins[76], H.-J. Mathes[40], J. Matthews[g], G. Matthiae[61,50], E. Mayotte[82], S. Mayotte[82], P.O. Mazur[d], G. Medina-Tanco[67], J. Meinert[37], D. Melo[7], A. Menshikov[39], C. Merx[40], S. Michal[31], M.I. Micheletti[5], L. Miramonti[58,48], M. Mogarkar[68], S. Mollerach[1], F. Montanet[35], L. Morejon[37], K. Mulrey[77,78], R. Mussa[51], W.M. Namasaka[37], S. Negi[31], L. Nellen[67], K. Nguyen[84], G. Nicora[9], M. Niechciol[43], D. Nitz[84], D. Nosek[30], A. Novikov[87], V. Novotny[30], L. Nožka[32], A. Nucita[55,47], L.A. Núñez[29], J. Ochoa[7,40], C. Oliveira[20], L. Östman[31], M. Palatka[31], J. Pallotta[9], S. Panja[31], G. Parente[76], T. Paulsen[37], J. Pawlowsky[37], M. Pech[31], J. Pękala[68], R. Pelayo[64], V. Pelgrims[14], L.A.S. Pereira[24], E.E. Pereira Martins[38,7], C. Pérez Bertolli[7,40], L. Perrone[55,47], S. Petrera[44,45], C. Petrucci[56], T. Pierog[40], M. Pimenta[70], M. Platino[7], B. Pont[77], M. Pourmohammad Shahvar[60,46], P. Privitera[86], C. Priyadarshi[68], M. Prouza[31], K. Pytel[69], S. Querchfeld[37], J. Rautenberg[37], D. Ravignani[7], J.V. Reginatto Akim[22], A. Reuzki[41], J. Ridky[31], F. Riehn[76,j], M. Risse[43], V. Rizi[56,45], E. Rodriguez[7,40], G. Rodriguez Fernandez[50], J. Rodriguez Rojo[11], S. Rossoni[42], M. Roth[40], E. Roulet[1], A.C. Rovero[4], A. Saftoiu[71], M. Saharan[77], F. Salamida[56,45], H. Salazar[63], G. Salina[50], P. Sampathkumar[40], N. San Martin[82], J.D. Sanabria Gomez[29], F. Sánchez[7], E.M. Santos[21], E. Santos[31], F. Sarazin[82], R. Sarmento[70], R. Sato[11], P. Savina[44,45], V. Scherini[55,47], H. Schieler[40], M. Schimassek[33], M. Schimp[37], D. Schmidt[40], O. Scholten[15,b], H. Schoorlemmer[77,78], P. Schovánek[31], F.G. Schröder[87,40], J. Schulte[41], T. Schulz[31], S.J. Sciutto[3], M. Scornavacche[7], A. Sedoski[7], A. Segreto[52,46], S. Sehgal[37], S.U. Shivashankara[73], G. Sigl[42], K. Simkova[15,14], F. Simon[39], R. Šmída[86], P. Sommers[e], R. Squartini[10], M. Stadelmaier[40,48,58], S. Stanič[73], J. Stasielak[68], P. Stassi[35], S. Strähnz[38], M. Straub[41], T. Suomijärvi[36], A.D. Supanitsky[7], Z. Svozilikova[31], K. Syrokvas[30], Z. Szadkowski[69], F. Tairli[13], M. Tambone[59,49], A. Tapia[28], C. Taricco[62,51], C. Timmermans[78,77], O. Tkachenko[31], P. Tobiska[31], C.J. Todero Peixoto[19], B. Tomé[70], A. Travaini[10], P. Travnicek[31], M. Tueros[3], M. Unger[40], R. Uzeiroska[37], L. Vaclavek[32], M. Vacula[32], I. Vaiman[44,45], J.F. Valdés Galicia[67], L. Valore[59,49], P. van Dillen[77,78], E. Varela[63], V. Vašíčková[37], A. Vásquez-Ramírez[29], D. Veberič[40], I.D. Vergara Quispe[3], S. Verpoest[87], V. Verzi[50], J. Vicha[31], J. Vink[80], S. Vorobiov[73], J.B. Vuta[31], C. Watanabe[27], A.A. Watson[c], A. Weindl[40], M. Weitz[37], L. Wiencke[82], H. Wilczyński[68], B. Wundheiler[7], B. Yue[37], A. Yushkov[31], E. Zas[76], D. Zavrtanik[73,74], M. Zavrtanik[74,73]

[1] Centro Atómico Bariloche and Instituto Balseiro (CNEA-UNCuyo-CONICET), San Carlos de Bariloche, Argentina
[2] Departamento de Física and Departamento de Ciencias de la Atmósfera y los Océanos, FCEyN, Universidad de Buenos Aires and CONICET, Buenos Aires, Argentina
[3] IFLP, Universidad Nacional de La Plata and CONICET, La Plata, Argentina
[4] Instituto de Astronomía y Física del Espacio (IAFE, CONICET-UBA), Buenos Aires, Argentina
[5] Instituto de Física de Rosario (IFIR) – CONICET/U.N.R. and Facultad de Ciencias Bioquímicas y Farmacéuticas U.N.R., Rosario, Argentina
[6] Instituto de Tecnologías en Detección y Astropartículas (CNEA, CONICET, UNSAM), and Universidad Tecnológica Nacional – Facultad Regional Mendoza (CONICET/CNEA), Mendoza, Argentina
[7] Instituto de Tecnologías en Detección y Astropartículas (CNEA, CONICET, UNSAM), Buenos Aires, Argentina
[8] International Center of Advanced Studies and Instituto de Ciencias Físicas, ECyT-UNSAM and CONICET, Campus Miguelete – San Martín, Buenos Aires, Argentina
[9] Laboratorio Atmósfera – Departamento de Investigaciones en Láseres y sus Aplicaciones – UNIDEF (CITEDEF-CONICET), Argentina
[10] Observatorio Pierre Auger, Malargüe, Argentina
[11] Observatorio Pierre Auger and Comisión Nacional de Energía Atómica, Malargüe, Argentina
[12] Universidad Tecnológica Nacional – Facultad Regional Buenos Aires, Buenos Aires, Argentina
[13] University of Adelaide, Adelaide, S.A., Australia
[14] Université Libre de Bruxelles (ULB), Brussels, Belgium
[15] Vrije Universiteit Brussels, Brussels, Belgium
[16] Centro Brasileiro de Pesquisas Fisicas, Rio de Janeiro, RJ, Brazil
[17] Centro Federal de Educação Tecnológica Celso Suckow da Fonseca, Petropolis, Brazil
[18] Instituto Federal de Educação, Ciência e Tecnologia do Rio de Janeiro (IFRJ), Brazil
[19] Universidade de São Paulo, Escola de Engenharia de Lorena, Lorena, SP, Brazil
[20] Universidade de São Paulo, Instituto de Física de São Carlos, São Carlos, SP, Brazil
[21] Universidade de São Paulo, Instituto de Física, São Paulo, SP, Brazil
[22] Universidade Estadual de Campinas (UNICAMP), IFGW, Campinas, SP, Brazil
[23] Universidade Estadual de Feira de Santana, Feira de Santana, Brazil
[24] Universidade Federal de Campina Grande, Centro de Ciencias e Tecnologia, Campina Grande, Brazil
[25] Universidade Federal do ABC, Santo André, SP, Brazil
[26] Universidade Federal do Paraná, Setor Palotina, Palotina, Brazil
[27] Universidade Federal do Rio de Janeiro, Instituto de Física, Rio de Janeiro, RJ, Brazil
[28] Universidad de Medellín, Medellín, Colombia
[29] Universidad Industrial de Santander, Bucaramanga, Colombia
[30] Charles University, Faculty of Mathematics and Physics, Institute of Particle and Nuclear Physics, Prague, Czech Republic
[31] Institute of Physics of the Czech Academy of Sciences, Prague, Czech Republic
[32] Palacky University, Olomouc, Czech Republic
[33] CNRS/IN2P3, IJCLab, Université Paris-Saclay, Orsay, France
[34] Laboratoire de Physique Nucléaire et de Hautes Energies (LPNHE), Sorbonne Université, Université de Paris, CNRS-IN2P3, Paris, France
[35] Univ. Grenoble Alpes, CNRS, Grenoble Institute of Engineering Univ. Grenoble Alpes, LPSC-IN2P3, 38000 Grenoble, France
[36] Université Paris-Saclay, CNRS/IN2P3, IJCLab, Orsay, France
[37] Bergische Universität Wuppertal, Department of Physics, Wuppertal, Germany
[38] Karlsruhe Institute of Technology (KIT), Institute for Experimental Particle Physics, Karlsruhe, Germany
[39] Karlsruhe Institute of Technology (KIT), Institut für Prozessdatenverarbeitung und Elektronik, Karlsruhe, Germany
[40] Karlsruhe Institute of Technology (KIT), Institute for Astroparticle Physics, Karlsruhe, Germany
[41] RWTH Aachen University, III. Physikalisches Institut A, Aachen, Germany
[42] Universität Hamburg, II. Institut für Theoretische Physik, Hamburg, Germany
[43] Universität Siegen, Department Physik – Experimentelle Teilchenphysik, Siegen, Germany
[44] Gran Sasso Science Institute, L'Aquila, Italy
[45] INFN Laboratori Nazionali del Gran Sasso, Assergi (L'Aquila), Italy
[46] INFN, Sezione di Catania, Catania, Italy
[47] INFN, Sezione di Lecce, Lecce, Italy
[48] INFN, Sezione di Milano, Milano, Italy
[49] INFN, Sezione di Napoli, Napoli, Italy
[50] INFN, Sezione di Roma "Tor Vergata", Roma, Italy
[51] INFN, Sezione di Torino, Torino, Italy

PoS(ICRC2025)965

[52] Istituto di Astrofisica Spaziale e Fisica Cosmica di Palermo (INAF), Palermo, Italy
[53] Osservatorio Astrofisico di Torino (INAF), Torino, Italy
[54] Politecnico di Milano, Dipartimento di Scienze e Tecnologie Aerospaziali , Milano, Italy
[55] Università del Salento, Dipartimento di Matematica e Fisica "E. De Giorgi", Lecce, Italy
[56] Università dell'Aquila, Dipartimento di Scienze Fisiche e Chimiche, L'Aquila, Italy
[57] Università di Catania, Dipartimento di Fisica e Astronomia "Ettore Majorana", Catania, Italy
[58] Università di Milano, Dipartimento di Fisica, Milano, Italy
[59] Università di Napoli "Federico II", Dipartimento di Fisica "Ettore Pancini", Napoli, Italy
[60] Università di Palermo, Dipartimento di Fisica e Chimica "E. Segrè", Palermo, Italy
[61] Università di Roma "Tor Vergata", Dipartimento di Fisica, Roma, Italy
[62] Università Torino, Dipartimento di Fisica, Torino, Italy
[63] Benemérita Universidad Autónoma de Puebla, Puebla, México
[64] Unidad Profesional Interdisciplinaria en Ingeniería y Tecnologías Avanzadas del Instituto Politécnico Nacional (UPIITA-IPN), México, D.F., México
[65] Universidad Autónoma de Chiapas, Tuxtla Gutiérrez, Chiapas, México
[66] Universidad Michoacana de San Nicolás de Hidalgo, Morelia, Michoacán, México
[67] Universidad Nacional Autónoma de México, México, D.F., México
[68] Institute of Nuclear Physics PAN, Krakow, Poland
[69] University of Łódź, Faculty of High-Energy Astrophysics,Łódź, Poland
[70] Laboratório de Instrumentação e Física Experimental de Partículas – LIP and Instituto Superior Técnico – IST, Universidade de Lisboa – UL, Lisboa, Portugal
[71] "Horia Hulubei" National Institute for Physics and Nuclear Engineering, Bucharest-Magurele, Romania
[72] Institute of Space Science, Bucharest-Magurele, Romania
[73] Center for Astrophysics and Cosmology (CAC), University of Nova Gorica, Nova Gorica, Slovenia
[74] Experimental Particle Physics Department, J. Stefan Institute, Ljubljana, Slovenia
[75] Universidad de Granada and C.A.F.P.E., Granada, Spain
[76] Instituto Galego de Física de Altas Enerxías (IGFAE), Universidade de Santiago de Compostela, Santiago de Compostela, Spain
[77] IMAPP, Radboud University Nijmegen, Nijmegen, The Netherlands
[78] Nationaal Instituut voor Kernfysica en Hoge Energie Fysica (NIKHEF), Science Park, Amsterdam, The Netherlands
[79] Stichting Astronomisch Onderzoek in Nederland (ASTRON), Dwingeloo, The Netherlands
[80] Universiteit van Amsterdam, Faculty of Science, Amsterdam, The Netherlands
[81] Case Western Reserve University, Cleveland, OH, USA
[82] Colorado School of Mines, Golden, CO, USA
[83] Department of Physics and Astronomy, Lehman College, City University of New York, Bronx, NY, USA
[84] Michigan Technological University, Houghton, MI, USA
[85] New York University, New York, NY, USA
[86] University of Chicago, Enrico Fermi Institute, Chicago, IL, USA
[87] University of Delaware, Department of Physics and Astronomy, Bartol Research Institute, Newark, DE, USA

[a] Max-Planck-Institut für Radioastronomie, Bonn, Germany
[b] also at Kapteyn Institute, University of Groningen, Groningen, The Netherlands
[c] School of Physics and Astronomy, University of Leeds, Leeds, United Kingdom
[d] Fermi National Accelerator Laboratory, Fermilab, Batavia, IL, USA
[e] Pennsylvania State University, University Park, PA, USA
[f] Colorado State University, Fort Collins, CO, USA
[g] Louisiana State University, Baton Rouge, LA, USA
[h] now at Graduate School of Science, Osaka Metropolitan University, Osaka, Japan
[i] Institut universitaire de France (IUF), France
[j] now at Technische Universität Dortmund and Ruhr-Universität Bochum, Dortmund and Bochum, Germany

Acknowledgments

The successful installation, commissioning, and operation of the Pierre Auger Observatory would not have been possible without the strong commitment and effort from the technical and administrative staff in Malargüe. We are very grateful to the following agencies and organizations for financial support:

Argentina – Comisión Nacional de Energía Atómica; Agencia Nacional de Promoción Científica y Tecnológica (ANPCyT); Consejo Nacional de Investigaciones Científicas y Técnicas (CONICET); Gobierno de la Provincia de

Mendoza; Municipalidad de Malargüe; NDM Holdings and Valle Las Leñas; in gratitude for their continuing cooperation over land access; Australia – the Australian Research Council; Belgium – Fonds de la Recherche Scientifique (FNRS); Research Foundation Flanders (FWO), Marie Curie Action of the European Union Grant No. 101107047; Brazil – Conselho Nacional de Desenvolvimento Científico e Tecnológico (CNPq); Financiadora de Estudos e Projetos (FINEP); Fundação de Amparo à Pesquisa do Estado de Rio de Janeiro (FAPERJ); São Paulo Research Foundation (FAPESP) Grants No. 2019/10151-2, No. 2010/07359-6 and No. 1999/05404-3; Ministério da Ciência, Tecnologia, Inovações e Comunicações (MCTIC); Czech Republic – GACR 24-13049S, CAS LQ100102401, MEYS LM2023032, CZ.02.1.01/0.0/0.0/16_013/0001402, CZ.02.1.01/0.0/0.0/18_046/0016010 and CZ.02.1.01/0.0/0.0/17_049/0008422 and CZ.02.01.01/00/22_008/0004632; France – Centre de Calcul IN2P3/CNRS; Centre National de la Recherche Scientifique (CNRS); Conseil Régional Ile-de-France; Département Physique Nucléaire et Corpusculaire (PNC-IN2P3/CNRS); Département Sciences de l'Univers (SDU-INSU/CNRS); Institut Lagrange de Paris (ILP) Grant No. LABEX ANR-10-LABX-63 within the Investissements d'Avenir Programme Grant No. ANR-11-IDEX-0004-02; Germany – Bundesministerium für Bildung und Forschung (BMBF); Deutsche Forschungsgemeinschaft (DFG); Finanzministerium Baden-Württemberg; Helmholtz Alliance for Astroparticle Physics (HAP); Helmholtz-Gemeinschaft Deutscher Forschungszentren (HGF); Ministerium für Kultur und Wissenschaft des Landes Nordrhein-Westfalen; Ministerium für Wissenschaft, Forschung und Kunst des Landes Baden-Württemberg; Italy – Istituto Nazionale di Fisica Nucleare (INFN); Istituto Nazionale di Astrofisica (INAF); Ministero dell'Università e della Ricerca (MUR); CETEMPS Center of Excellence; Ministero degli Affari Esteri (MAE), ICSC Centro Nazionale di Ricerca in High Performance Computing, Big Data and Quantum Computing, funded by European Union NextGenerationEU, reference code CN_00000013; México – Consejo Nacional de Ciencia y Tecnología (CONACYT) No. 167733; Universidad Nacional Autónoma de México (UNAM); PAPIIT DGAPA-UNAM; The Netherlands – Ministry of Education, Culture and Science; Netherlands Organisation for Scientific Research (NWO); Dutch national e-infrastructure with the support of SURF Cooperative; Poland – Ministry of Education and Science, grants No. DIR/WK/2018/11 and 2022/WK/12; National Science Centre, grants No. 2016/22/M/ST9/00198, 2016/23/B/ST9/01635, 2020/39/B/ST9/01398, and 2022/45/B/ST9/02163; Portugal – Portuguese national funds and FEDER funds within Programa Operacional Factores de Competitividade through Fundação para a Ciência e a Tecnologia (COMPETE); Romania – Ministry of Research, Innovation and Digitization, CNCS-UEFISCDI, contract no. 30N/2023 under Romanian National Core Program LAPLAS VII, grant no. PN 23 21 01 02 and project number PN-III-P1-1.1-TE-2021-0924/TE57/2022, within PNCDI III; Slovenia – Slovenian Research Agency, grants P1-0031, P1-0385, I0-0033, N1-0111; Spain – Ministerio de Ciencia e Innovación/Agencia Estatal de Investigación (PID2019-105544GB-I00, PID2022-140510NB-I00 and RYC2019-027017-I), Xunta de Galicia (CIGUS Network of Research Centers, Consolidación 2021 GRC GI-2033, ED431C-2021/22 and ED431F-2022/15), Junta de Andalucía (SOMM17/6104/UGR and P18-FR-4314), and the European Union (Marie Sklodowska-Curie 101065027 and ERDF); USA – Department of Energy, Contracts No. DE-AC02-07CH11359, No. DE-FR02-04ER41300, No. DE-FG02-99ER41107 and No. DE-SC0011689; National Science Foundation, Grant No. 0450696, and NSF-2013199; The Grainger Foundation; Marie Curie-IRSES/EPLANET; European Particle Physics Latin American Network; and UNESCO.